JOURNAL OF CATALYSIS **161,** 31–42 (1996)
ARTICLE NO. 0159

Transient Kinetic Study of the Oxidation and Hydrogenation of Carbon Species Formed during CH_4/He, CO_2/He, and CH_4/CO_2 Reactions over Rh/Al_2O_3 Catalyst

V. A. Tsipouriari, A. M. Efstathiou, and X. E. Verykios

Department of Chemical Engineering and Institute of Chemical Engineering and High Temperature Chemical Processes, University of Patras, P.O. Box 1414, GR-26500 Patras, Greece

Received July 26, 1995; revised January 31, 1996; accepted February 1, 1996

The dissociation of CH_4 and CO_2 on 0.5 wt% Rh/Al_2O_3 catalyst has been investigated at 650°C using transient techniques with on-line mass spectrometry. The dissociation of CH_4 results in the formation of large amounts of gaseous H_2 and carbonaceous species (C_xH_y, $y \cong 0$) on the surface after 10 min of reaction. Oxidation of these carbon species to CO_2 proceeds with an intrinsic activation energy of 63 kJ mol^{-1}, while hydrogenation to CH_4 with an intrinsic activation energy of the order of 240 kJ mol^{-1}. On the other hand, dissociation of CO_2 results in the formation of much lower quantities of carbon species under the same reaction conditions. In this case, two kinds of carbon species were identified. Hydrogenation of the main carbon species proceeds with an activation energy of 96 kJ mol^{-1}, while its oxidation proceeds with significantly different kinetics than the carbon derived from CH_4 dissociation. Characterization of carbon accumulated on the catalyst surface during reforming reaction of CH_4 with CO_2 has also been performed. It was found that this carbon mostly originates from the CO_2 molecule and it is significantly more reactive than the carbon derived from CH_4 decomposition, but of similar reactivity as the carbon derived from CO_2 dissociation. Temperature-programmed hydrogenation (TPH) experiments of the carbonaceous species formed during reforming reaction at 650°C revealed three different kinds of carbon species. The carbon species with the largest quantity hydrogenated to CH_4, according to the TPH response, is found to be associated with an intrinsic activation energy of 125 kJ mol^{-1} for its hydrogenation process.

INTRODUCTION

We have recently reported on two studies concerning (a) the effects of support and Rh crystallite size on activity and deactivation characteristics and (b) mechanistic aspects of the carbon and oxygen reaction pathways of the formation of CO, for the reforming of methane with carbon dioxide to synthesis gas over supported Rh catalysts (1, 2). The initial specific activity of Rh catalysts was found to depend strongly on the carrier employed to disperse the metal, decreasing in the order: yttria-stabilized zirconia (YSZ) > $Al_2O_3 \geq TiO_2 > SiO_2 > La_2O_3 > MgO$. Both activity and rate of deactivation were found to decrease with increasing Rh particle size (1). In addition, the degree of these dependencies was found to be largely affected by the nature of the carrier, suggesting that the dependence of activity and rate of deactivation on metal particle size is likely related to metal–support interactions. Evidence was presented that carbon deposition, metal-sintering, and poisoning of surface Rh sites by species originating from the carrier contribute to catalyst deactivation under reforming reaction at 650°C (1).

Steady-state tracing techniques (use of $^{13}CH_4$, $^{13}CO_2$, and $C^{18}O_2$) have been applied to measure the surface coverage of adsorbed active carbon- and oxygen-containing reaction intermediate species which are found in the reaction pathway of CO formation over Rh/Al_2O_3 and Rh/YSZ catalysts under reforming reaction at 650°C (2). It was found that CH_x species, originating from methane decomposition, are more active toward oxidation to CO (their surface coverage was immeasurable) than carbon species originating from the CO_2 molecule. In particular, inactive carbonaceous species originating from the CO_2 molecule accumulate on the surface of Rh/Al_2O_3 during reforming reaction at 650°C (2). It was also shown that lattice oxygen species of the YSZ carrier migrate onto the Rh surface of Rh/YSZ catalyst and react with carbon-containing species to form CO. It was suggested that this reaction route could explain the highest specific activity exhibited by Rh/YSZ as compared to the other supported Rh catalysts investigated (1, 3).

Carbon deposition on the catalyst surface during the reforming reaction of CH_4 with CO_2 must be avoided for industrial scale applications. The kinetics of carbon deposition on reforming catalysts and its reactivity toward oxidation or hydrogenation are important technological aspects. Although there is a large amount of work related to these aspects over steam reforming catalysts (4), there is lack of information concerning CO_2 reforming catalysts and, especially, supported Rh catalysts. Recently, Claridge *et al.* (5) have addressed these issues for catalysts of the partial oxidation of methane to synthesis gas. Our recent work

0021-9517/96 $18.00

(1–3) on reforming reaction of CH_4 with CO_2 over supported Rh catalysts, outlined in the previous paragraphs, has addressed quantitatively the amount of active and inactive carbon accumulated during CO_2 reforming reaction at 650°C over some supported Rh catalysts.

Erdöhelyi *et al.* (6) have studied the dissociation of CH_4 and CO_2, as well as the reforming reaction of CH_4 with CO_2, in the temperature range of 20–500°C over supported Rh catalysts. The authors have shown that supported Rh is active in the decomposition of CH_4 to give H_2, a small amount of C_2H_6, and carbonaceous residues. Three different kinds of carbon were distinguished, following CH_4 decomposition, by means of the H_2 TPR technique. The reactivity of each kind of carbon was found to depend on reaction temperature and time on stream in CH_4/He mixture (6). After 1 h of reforming reaction of CH_4 with CO_2 at 500°C, only a small amount of carbon ($\theta_c = 0.06$) was accumulated on the surface of the 1 wt% Rh/Al_2O_3 catalyst.

The present work reports comparative kinetic results of the transient hydrogenation and oxidation of carbonaceous species accumulated on the surface of the Rh/Al_2O_3 catalyst following reaction at 650°C with CH_4/He, CO_2/He, and CH_4/CO_2/He mixtures. The various kinds of transient experiments performed with on-line mass spectrometry, and the kinetic model developed to interpret the results obtained, probe for large differences in the chemical structure, reactivity and kinetics of hydrogenation, and oxidation of the carbonaceous species formed after either CH_4 decomposition, CO_2 dissociation, or CH_4/CO_2 reaction to synthesis gas. The present study confirms previous results (2, 3) concerning the origin of the carbon accumulated during reforming reaction at 650°C (CH_4 vs CO_2 molecular route).

EXPERIMENTAL

(a) Preparation and Characterization of Rh/Al_2O_3 Catalyst

A 0.5 wt% Rh/γ-Al_2O_3 catalyst was prepared by impregnating γ-Al_2O_3 (Akzo Chemicals) to incipient wetness with an aqueous solution of $RhCl_3 \cdot 3H_2O$ (Alfa Products). The solid was then dried at 110°C in an oven for 24 h. For storage it was passivated by H_2 reduction at 200°C for 2 h. Details of the preparation procedure have been reported previously (1).

In every kind of transient reaction studied, for example temperature-programmed hydrogenation (TPH) and temperature-programmed oxidation (TPO) following reaction with CH_4/He, CO_2/He, and CH_4/CO_2/He mixtures, a fresh catalyst sample (0.5 g) was used. This was first reduced under hydrogen flow at 500°C for 2 h and then treated with He for 2 h at 650°C to obtain a fairly stabilized metal surface area for subsequent experiments. Following a given oxidation (i.e., TPO or isothermal) or hydrogenation (i.e., TPH or isothermal) treatment, a hydrogen reduction treatment with 1 bar H_2 at 500°C between $\frac{1}{2}$ and 1 h was applied. Then the catalyst sample was brought to reaction conditions under He flow. Following a given isothermal oxidation experiment performed at $T < 500$°C, the catalyst temperature was then increased to 500°C under O_2/He flow in order to completely remove any carbonaceous species left on the surface.

The BET surface area of the alumina support, as well as the metal surface area were measured in a constant volume, high-vacuum adsorption apparatus (Micrometrics Accusorb 2100E) following the BET method with argon adsorption and the method of extrapolation of the linear part of the H_2 chemisorption isotherm at 25°C to zero pressure, respectively. The support surface area was found to be 100 m^2/g. The active metal surface was found to be 48.6 μmol Rh surface atoms/g of catalyst, assuming $H/Rh_s = 1.0$, and the average Rh particle size was estimated to be 1.1 nm, assuming spherical particles. The fraction of the Rh metal exposed after the fresh sample was treated with He or CH_4/CO_2/He gases at 650°C for 2 h, was found to be 0.22, yielding an average Rh particle size of 4.5 nm (1).

(b) Reactor–Flow System for Transient Studies

The reactor used in this study consists of two 4.0-mm-i.d. sections of quartz tubes which serve as inlet and outlet to and from a quartz cell of 7.0 mm i.d. (nominal volume 2 ml). The entrance to the reactor cell was machined in such a way as to create local gas mixing. Heating was provided by a small furnace controlled by a programmable temperature controller (Omega Engineering Inc., CN-2010). The temperature of the catalyst is measured by a K-type thermocouple placed within a quartz capillary well in the middle of the catalyst bed.

An appropriate flow system that allows for the application of transient methods (abrupt switches in the feed gas composition) was employed in the present investigation. The main design features of this system has been described in detail elsewhere (7). Analysis of the gases during transients is done by on-line mass spectrometer (VG Quadrupoles, Sensorlab 200D) equipped with a fast response inlet capillary/leak diaphragm system. The desired gas mixtures are made up in a separate preparation apparatus and not by continuous blending of two or more streams. Calibration of the mass spectrometer is performed based on a prepared mixture of a known composition. The output signal from the mass spectrometer detector is then converted to mole fraction by appropriate software. The integrity of the transient results, free of any flow disturbances, was maintained as described (7–9). Methane transients were recorded at $m/z = 15$, while H_2, CO, and CO_2 transients at $m/z = 2$, 28, and 44, respectively. For the measurement of CO ($m/z = 28$) in the presence of CO_2, the contribution of

CO_2 to the 28 peak was found to be such that the intensity ratio 28/44 for CO_2 was 0.12.

The CH_4/CO_2/He mixture was prepared with a composition of 20% CH_4, 20% CO_2, and 60% He. The flow rate of all gases was 30 ml/min (ambient). At this flow rate the mean residence time in the reactor cell containing the catalyst bed was approximately 2 s. The H_2 and He gases used were standard (99.95%) and ultrahigh purity (99.999%), respectively. Further purification of these gases was performed by using molecular sieve (13X) and MnO_x traps for removing traces of water and oxygen, respectively.

RESULTS

Various transient experiments were conducted in order to study (qualitatively and quantitatively) the chemical interaction of CH_4 and CO_2 molecules with the surface of Rh supported on Al_2O_3, either individually or in mixture, in which case the methane reforming reaction takes place. In particular, transient hydrogenation and oxidation experiments of the carbon species formed during these interactions have been conducted, from which useful information was obtained via kinetic modeling.

(a) CH_4/He Reaction

Figure 1 shows the transient response of H_2 production after a switch from He to 20% CH_4/He at 650°C is made over a freshly reduced Rh/Al_2O_3 sample. Hydrogen was the only gaseous species observed (no higher hydrocarbons and neither CO nor CO_2 were observed). After passing CH_4/He over the reduced Rh surface, the rate of dissociation of CH_4 to hydrogen and carbonaceous species (CH_x) is high (TOF = 0.045 s^{-1}, overshoot at $t = 0$), while afterward it decays slowly. The latter result is due to the decrease of concentration of active Rh sites, because of carbon accumulation, as indicated below. After 10 min on stream the rate of H_2 production is found to be about seven times lower than the initial rate (overshoot at $t = 0$, Fig. 1).

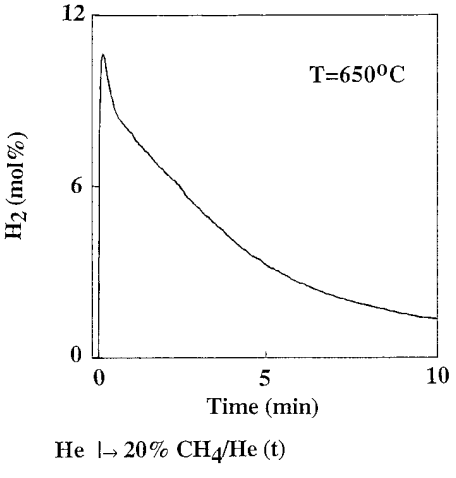

FIG. 1. Transient isothermal response of H_2 production at 650°C after the switch: He → 20% CH_4/He (t) is made over the 0.5 wt% Rh/Al_2O_3 catalyst.

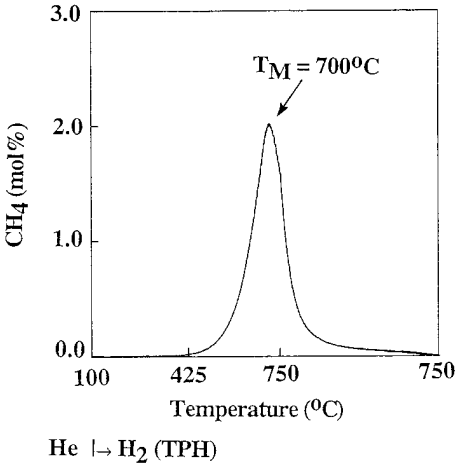

FIG. 2. Temperature-programmed hydrogenation (TPH) of adsorbed carbonaceous species formed during the first 10 min of the 20% CH_4/He reaction at 650°C over the 0.5 wt% Rh/Al_2O_3 catalyst. $W = 0.5$ g; $Q =$ 30 ml/min (ambient); $\beta = 20$°C/min.

Figure 2 shows results of a temperature-programmed hydrogenation (TPH) experiment of carbon species formed during CH_4/He reaction (Fig. 1) according to the following gas delivery sequence: After reaction of CH_4/He on the Rh/Al_2O_3 catalyst at 650°C for 10 min (Fig. 1), the feed was changed to pure He at 650°C for 10 min, followed by cooling of the reactor under He flow to 100°C. The feed was then changed to pure H_2 and the temperature of the catalyst was increased at the rate of 20°C/min to 750°C in order to carry out a TPH experiment. Note that at the end of the 10-min He purge of the reactor at 650°C, neither CO_2 nor CH_4 were detected. There is a main CH_4 peak shown in Fig. 2 which is centered at 700°C, tailing out to 750°C. Integration of the CH_4 response shown in Fig. 2 results in an equivalent amount of carbon of 395 μmol/g, or θ_c of 8.1 monolayers ($C/Rh_s = 1$).

An estimate of the average chemical composition of the carbonaceous species deposited on the catalyst surface, which were measured by the TPH experiment described in Fig. 2, can be made based on the results of Figs. 1 and 2. From the H_2 transient response shown in Fig. 1 it is estimated that during 10 min of CH_4/He reaction the amount of H_2 produced is 825 μmol H_2/g. The amount of equivalent carbon deduced from the TPH experiment is 395 μmol C/g, which corresponds to an equivalent amount of 395 μmol CH_4/g consumed; note that the hydrogen material balance is within 5%. These results then lead to the conclusion that the hydrogen content of the carbonaceous species, C_xH_y, which accumulate on Rh/Al_2O_3 during exposure to CH_4/He gas mixture is practically zero.

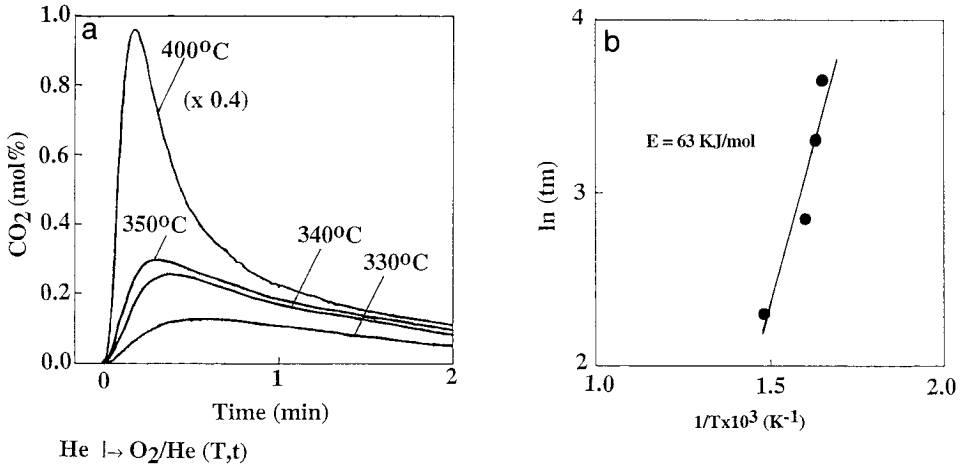

FIG. 3. (a) Transient isothermal responses of CO_2 formation obtained after the following gas delivery sequence is applied: 20% CH_4/He (650°C, 10 min) → He (650°C, 10 min) → cool down in He flow to T → 10% O_2/He (T, t). (b) Plot of ln (t_m) vs $1/T$ according to Eq. [8] and the results obtained in (a); t_m is the time of appearance of peak maximum in the rate of CO_2 formation under O_2/He flow for the conditions of the experiments given in (a).

The reactivity of carbonaceous species formed during CH_4/He reaction toward oxidation was also investigated as follows: After the catalyst was exposed to 20% CH_4/He mixture at 650°C for 10 min, the feed was changed to He for 10 min at 650°C. The reactor was then cooled in He flow to a certain temperature, following which the feed was changed to 10% O_2/He mixture to carry out a transient isothermal oxidation experiment. Figure 3a shows CO_2 gas-phase transient response curves obtained during the isothermal oxidation step at temperatures in the range of 330–400°C. As the temperature of oxidation increases, the peak maximum of the CO_2 response shifts toward smaller times on stream in O_2/He mixture, while, at the same time, the maximum rate of CO_2 production increases. These kinetic features of the present oxidation reaction of carbonaceous species to CO_2 can be modeled to obtain useful kinetic parameters. The kinetic model developed for the present case is described below.

It is assumed that the chemisorption of O_2 during the transient isothermal oxidation experiment is described by the following elementary step,

$$O_2(g) + 2(s) \rightleftharpoons 2O\text{-}s, \qquad [1]$$

where (s) is an active Rh surface site. The surface coverage of adsorbed oxygen species, $\theta_{O\text{-}s}$, is assumed to remain constant during the experiment. It is also assumed that the oxidation of CH_x species (in the present case $x \cong 0$), derived from the CH_4/He reaction (Figs. 1 and 2), proceeds via the sequence of the following two elementary steps:

$$CH_x + O\text{-}s \xrightarrow{k_1} CO\text{-}s + xH \qquad [2]$$

$$CO\text{-}s + O\text{-}s \xrightarrow{k_2} CO_2 + 2(s). \qquad [3]$$

The rate of CO_2 production is then given by

$$R_{CO_2} = k_2 \cdot \Theta_{CO\text{-}s} \cdot \Theta_{O\text{-}s}. \qquad [4]$$

Unsteady-state material balance equations for the CH_x and CO-s adsorbed species, based on reaction steps [2] and [3], lead to an equation for the rate of CO_2 production,

$$R_{CO_2} = \frac{k_1 \cdot k_2 \cdot \Theta_{O\text{-}s} \cdot \Theta^{o}_{CH_x}}{k_1 - k_2} \cdot [\exp(-k_2 \cdot \Theta_{O\text{-}s} \cdot t) - \exp(-k_1 \cdot \Theta_{O\text{-}s} \cdot t)], \qquad [5]$$

where $\Theta^{o}_{CH_x}$ is the initial amount of CH_x species, before the isothermal transient oxidation experiment. Details of the material balance equations are given in the Appendix.

The time of appearance of the maximum of the rate of CO_2 production, t_m, is obtained by differentiation of Eq. [5]:

$$t_m = \ln\left(\frac{k_2}{k_1}\right) \Big/ (k_2 - k_1) \cdot \Theta_{O\text{-}s}. \qquad [6]$$

After substituting the relationship: $k_2 = \alpha k_1$ (at $T = \text{const}$), where α is a real number smaller or larger than unity, into Eq. [6], the following equation is obtained:

$$t_m = \frac{\ln(\alpha)}{\Theta_{O\text{-}s} \cdot k_1(\alpha - 1)}. \qquad [7]$$

Upon introduction of the Arrhenius relationship for the rate constant, Eq. [7] can be rearranged to give

$$\ln(t_m) = \ln(\gamma) + \left(\frac{E}{R}\right)\left(\frac{1}{T}\right), \qquad [8]$$

where γ is a constant and E is the intrinsic activation energy of the rate-determining step. The significance of the value of

α in determining whether step [2] or [3] is the rate-limiting step is discussed in the Appendix.

The values of t_m obtained from the experiments described in Fig. 3a were used in Eq. [8] and corresponding results ($\ln(t_m)$ vs $1/T$) are plotted in Fig. 3b. A good fit to the model described above is obtained, from which an intrinsic activation energy (63 kJ/mol) of the rate-limiting step is estimated.

The hydrogenation kinetics of the carbon formed upon CH_4/He reaction at 650°C was studied as follows: The 20% CH_4/He mixture was passed over the catalyst for 10 min at 650°C followed by a 10-min He purge. The reactor was subsequently cooled in He flow to a certain temperature, the feed was changed to pure H_2, while, at the same time, transient isothermal responses were monitored by mass spectrometry. The only product of hydrogenation was found to be methane and results are given in Fig. 4 for the temperatures of 520 and 575°C. After the switch to H_2, an initial rapid increase in the rate of hydrogenation is observed, while, afterward (within 30 s), it decays to a much lower value. For longer times on stream there is a slow decrease of the hydrogenation rate. In contrast to the case of isothermal oxidation presented in Fig. 3a, where a shift of the peak maximum of CO_2 response with temperature is observed, no such a shift is observed in the case of isothermal hydrogenation (first sharp peak at $t = 0$, Fig. 4) in the range of 500–700°C. This result can be associated with certain kinetic features of the hydrogenation process of the carbon species which are discussed later.

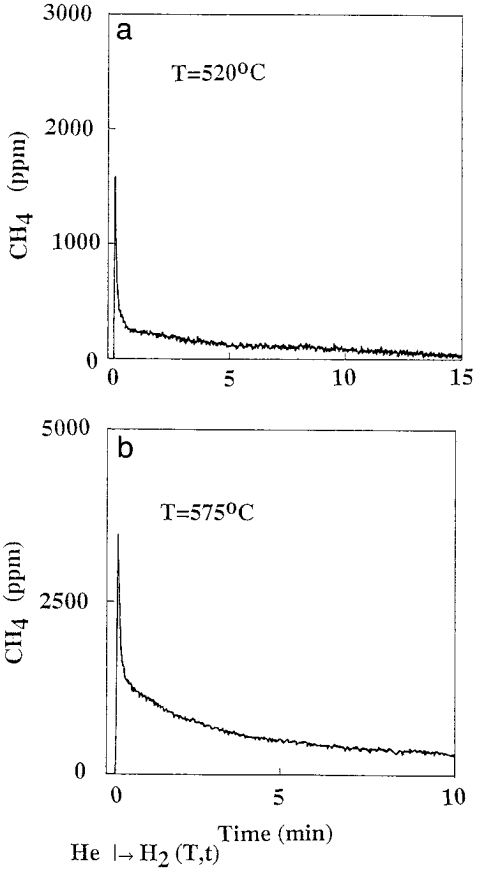

FIG. 4. Transient isothermal responses of CH_4 obtained after the following gas delivery sequence is applied: 20% CH_4/He (650°C, 10 min) → He (650°C, 10 min) → cool down in He flow to T → H_2 (T, t).

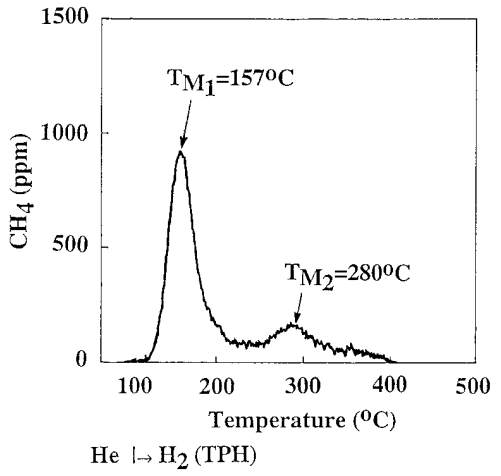

FIG. 5. Temperature-programmed hydrogenation (TPH) of adsorbed carbonaceous species formed during the first 10 min of the 20% CO_2/He reaction at 650°C over the 0.5 wt% Rh/Al_2O_3 catalyst. $W = 0.5$ g; $Q = 30$ ml/min (ambient); $\beta = 20$°C/min.

(b) CO_2/He Reaction

Figure 5 shows results of a TPH experiment of carbon species formed during CO_2/He reaction over the Rh/Al_2O_3 catalyst, similar to that presented in Fig. 2 in the case of CH_4/He reaction. Two well-resolved CH_4 peaks are observed, the first one centered at approximately 157°C and the second one at 280°C. The quantity of CH_4 which corresponds to the first peak is about four times larger than that of the second peak. The total amount of equivalent carbon corresponding to the CH_4 response shown in Fig. 5 is found to be 6.0 μmol/g, or $\theta_c = 0.12$.

Figure 6 shows the CO_2 response obtained during a TPO experiment of carbon species formed after treatment of the catalyst with a 20% CO_2/He mixture at 650°C for 10 min, as in the case of the TPH experiment presented in Fig. 5. Two kinds of carbon species are probed, based on the two CO_2 peaks observed ($T_{M_1} = 150$°C and $T_{M_2} = 280$°C). This result is similar to that obtained during the TPH experiment (Fig. 5). However, in the case of the TPO experiment, it is found that the amount of carbon removed as CO_2 is 18.0 μmol/g, or $\theta_c = 0.37$, a quantity three times larger than that obtained during the TPH experiment. Note that significant quantities of CO_2 appear to temperatures higher than 350°C during TPO (Fig. 6), while a very small CH_4 response is observed above 350°C during TPH (Fig. 5).

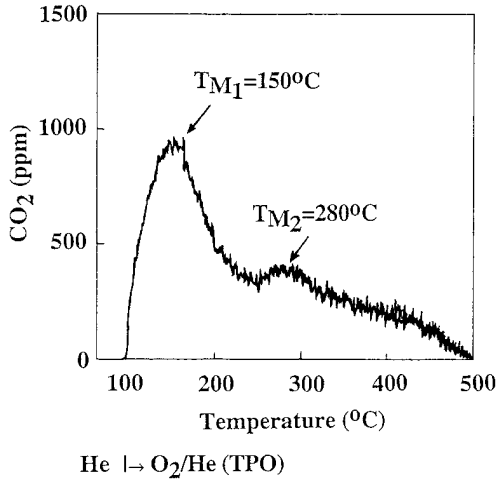

FIG. 6. Temperature-programmed oxidation (TPO) of adsorbed carbonaceous species formed during the first 10 min of the 20% CO_2/He reaction at 650°C over the 0.5 wt% Rh/Al_2O_3 catalyst. $W = 0.5$ g; $Q = 30$ ml/min (ambient); $\beta = 20$°C/min.

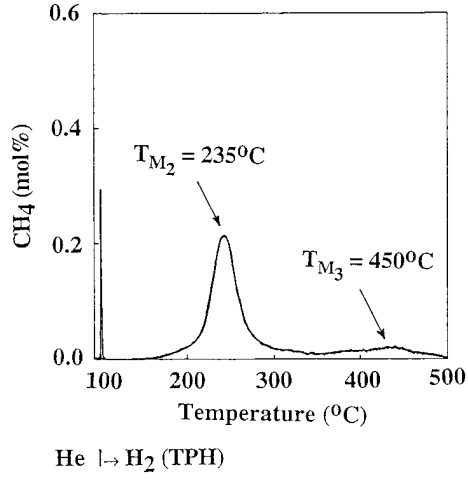

FIG. 7. Temperature-programmed hydrogenation (TPH) of adsorbed carbonaceous species formed during the first 10 min of the CH_4/CO_2/He (CO_2 reforming) reaction at 650°C over the 0.5 wt% Rh/Al_2O_3 catalyst. $W = 0.5$ g; $Q = 30$ ml/min (ambient); $\beta = 20$°C/min.

Transient isothermal oxidation experiments of carbon species formed at 650°C after 10 min of CO_2/He reaction were conducted at temperatures in the range of 250–450°C. The experimental procedure applied was similar to that described in relation to Fig. 3a in the case of CH_4/He reaction. An abrupt increase (spike at $t = 0$) in the rate of CO_2 formation was observed upon switching the feed to the O_2/He mixture. It was found that by varying the temperature of oxidation in the range of 250–450°C the peak maximum in the rate of CO_2 formation always appeared at times close to zero (spike at $t = 0$–3 s). This result is different than that observed in similar experiments for the oxidation of carbon derived from the CH_4/He reaction (Fig. 3a), and is related to differences in the intrinsic kinetics of oxidation, as discussed later.

(c) CH_4/CO_2/He Reaction

Figure 7 shows the CH_4 response versus temperature obtained during TPH of the carbon species formed after CH_4/CO_2/He reaction at 650°C for 10 min. In the present case, reforming reaction of CH_4 with CO_2 to synthesis gas occurs. At the conditions of the experiment, the CH_4 conversion is found to be 72%. The CH_4 response in Fig. 7 shows three well-resolved peaks which are assigned to three different kinds of carbon species, namely C_α, C_β, and C_γ which correspond to the reactivity order observed in the TPH spectrum of Fig. 7. The C_α carbon species is hydrogenated rapidly at low temperature (100°C), the C_β, the most abundant one, is hydrogenated in the range of 150–320°C, and the C_γ, the least active, in the range of 350–500°C. Similar TPH experiments as that shown in Fig. 7 were conducted for different times on stream in CH_4/CO_2/He mixture and the results obtained are summarized in Table 1. It is seen that up to 1 h of reforming reaction, the amount of carbon species formed is practically constant, while after 2 h of reaction the amount of carbon hydrogenated to CH_4 decreases by 40%. On the other hand, TPO experiments (not presented) revealed that the amount of carbon formed after CH_4/CO_2/He reaction at 650°C and up to 2 h on stream is about the same (the same amount of CO_2 is produced during TPO). These TPH and TPO results indicate that aging of carbon with time of reaction occurs and the aged carbon is inactive toward hydrogenation but active toward oxidation to CO_2.

The amount of carbon species accumulated on the surface of the Rh/Al_2O_3 catalyst was also determined at 550

TABLE 1

Amounts of Carbon Species Formed during CH_4/CO_2/He Reaction at 650°C as a Function of Time on Stream Determined by Temperature-Programmed Hydrogenation (TPH) Experiments (CH_4 Formation)

Time on stream	Carbon (μmol/g cat)			
	C_a	C_β	C_γ	C_{total}
2 min	0.7	15.6	1.9	18.2
	(0.015)[a]	(0.32)	(0.04)	(0.38)
10 min	0.4	11.7	2.4	14.5
	(0.008)	(0.24)	(0.05)	(0.3)
30 min	0.4	11.2	4.4	16.0
	(0.008)	(0.20)	(0.09)	(0.30)
1 h	0.5	10.6	4.0	15.1
	(0.01)	(0.20)	(0.08)	(0.29)
2 h	0.3	9.7	1.4	11.4
	(0.006)	(0.2)	(0.03)	(0.24)

[a] Numbers in parentheses represent the equivalent amount of carbon in monolayers of surface Rh ($C/Rh_s = 1$).

TABLE 2

Amount of Carbon Species Formed during CH_4/CO_2/He Reaction as a Function of Reaction Temperature and Time on Stream (Δt) Determined by Temperature-Programmed Oxidation (TPO) Experiments ($CO_2 + CO$ Formation)

	Carbon (μmol/g cat)	
T (°C)	$\Delta t = 10$ min	$\Delta t = 2$ h
550	26.3 (0.54)[a]	21.7 (0.45)
650	31.0 (0.64)	29.6 (0.61)
750	21.3 (0.43)	11.3 (0.23)

[a]Numbers in parentheses represent the equivalent amount of carbon in monolayers of surface Rh ($C/Rh_s = 1$).

and 750°C after 10 min and 2 h of reforming reaction by TPO experiments. The results obtained are presented in Table 2 along with corresponding ones obtained at 650°C as mentioned in the previous paragraph. Of importance is the fact that the amount of carbon accumulated decreases significantly when the reaction occurs at 750°C as compared to 650°C, and also when the reaction time increases from 10 min to 2 h.

Transient isothermal hydrogenation experiments of carbon species formed after CH_4/CO_2/He reaction at 650°C for 10 min are presented in Fig. 8. The experimental procedure applied was similar to that described with respect to Fig. 4. In the temperature range of 250–400°C, upon switching the feed from He to pure H_2 the rate of CH_4 formation goes through a maximum (spike at $t = 0$), while within 30 s on stream most of the carbon species is reacted off the catalyst surface. A similar behavior was observed in the case of isothermal oxidation of the carbon species to CO_2 in the temperature range of 350–450°C.

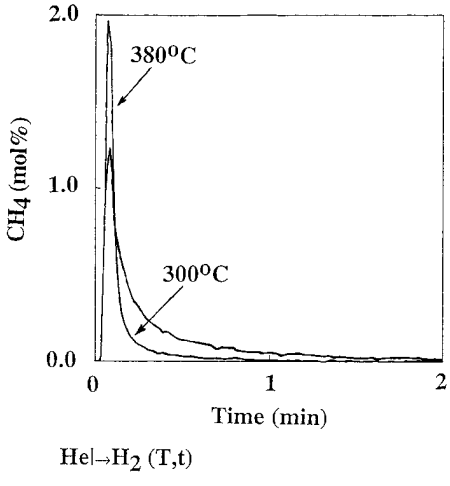

FIG. 8. Transient isothermal responses of CH_4 obtained after the following gas delivery sequence is applied: CH_4/CO_2/He (650°C, 10 min) → He (650°C, 10 min) → cool down in He flow to T → H_2 (T, t).

DISCUSSION

(a) Interaction of CH_4 with Rh

The transient results of Figs. 1 and 2, which describe the H_2 evolution and the reactivity of carbonaceous residues left on the catalyst surface after 10 min of CH_4/He exposure at 650°C, clearly illustrate that the rate of CH_4 decomposition at 650°C is very high (initial rate: 2.2 μmol/g · s, or TOF = 0.045 s^{-1}). As time on stream increases the initial rate of methane decomposition decays quickly to a low value (TOF = 0.007 s^{-1} after 10 min of reaction). This is very likely due to the decrease of the number of active Rh sites because of carbon accumulation (Fig. 2). However, in spite of the fact that after 10 min of reaction the amount of carbon accumulated on the catalyst surface is very high ($\theta_c = 8.1$), the dissociation of CH_4 still takes place. This result strongly suggests that the carbon formed cannot be atomically dispersed but is rather in the form of whiskers or graphite. Some of this carbon could also be found on the alumina surface, considering the high temperature of reaction (migration of carbon from Rh to the alumina surface). The latter could explain the occurrence of reaction for times longer than 10 min even though the equivalent amount of carbon formed largely exceeds the monolayer value. It is also clear from the results of Figs. 1 and 2 (see Results, section (a)) that decomposition of CH_4 at 650°C from a mixture containing 20 mol% CH_4 results in carbonaceous species deficient in hydrogen, C_α, a fraction of which are rapidly transformed into carbon in the form of whiskers and/or graphite, C_β, as already mentioned above. This process can be represented by elementary reaction steps,

$$CH_4(g) + 2(s) \rightarrow CH_3(s) + H(s) \quad [9]$$

$$CH_3(s) \rightarrow CH_x(s) + (3 - x)H(s) \quad [10]$$

$$CH_x(s) \rightarrow C(s) + xH(s) \quad [11]$$

$$C(s) \rightarrow C_\beta(s) \quad [12]$$

$$H(s) + H(s) \leftrightharpoons H_2(g), \quad [13]$$

where (s) represents an active Rh site.

Somewhat different results were obtained by Erdöhelyi *et al.* (6) who conducted similar experiments over a 1 wt% Rh/Al_2O_3 catalyst, however at temperatures significantly lower (200–300°C) than those employed in the present study. These authors observed formation of C_2H_6 upon interaction of CH_4 with the catalyst surface, which was not observed in the present study. It is conceivable that, in the present study, adsorbed CH_3 hydrocarbon species, which are initially formed according to reaction step [9], are

rapidly dehydrogenated to carbon, at the high temperature of 650°C, rather than to react to C_2H_6 by a coupling reaction step of two CH_3 species. In the TPH experiment, following decomposition of CH_4 at 250°C for 1 min, Erdöhelyi *et al.* (6) observed two methane peaks designated as C_α (active carbon) and C_β (less active carbon). The C_α carbon species was hydrogenated at 50°C, while the C_β species (the dominant one) appeared at $T_M = 175$°C. The authors also mention that the length and temperature of exposure influenced the distribution of carbon forms and their hydrogenation activity. In particular, when CH_4 decomposition occurred at 400–500°C the highly reactive C_α form was missing from the TPH spectrum and a significant proportion of the C_β form was transformed into a less reactive form, resulting in a CH_4 peak with $T_M = 605$°C. These results seem to agree with the TPH results of the present work (Fig. 2). When decomposition of CH_4 occurs at 650°C for 10 min a relatively inactive form of carbon is obtained ($T_M = 700$°C), suggesting that aging of the carbon produced occurs (reaction step [12]).

(b) Interaction of CO_2 with Rh

The interaction of CO_2 with the Rh/Al_2O_3 catalyst surface seems to be different than that of CH_4 with respect to carbon deposition, as revealed in the present work. The TPH and TPO results presented in Figs. 5 and 6, respectively, indicate that much lower quantities of carbonaceous species are deposited upon exposure of CO_2 to the catalyst surface at the same temperature (650°C), reaction time (10 min), and partial pressure ($P_{CH_4} = P_{CO_2} = 0.2$ bar). The only route for carbon deposition during CO_2/He exposure is that of the dissociation of adsorbed CO species as indicated below:

$$CO_2(g) + 2(s) \leftrightharpoons CO(s) + O(s) \quad [14]$$

$$CO(s) + (s) \leftrightharpoons C(s) + O(s) \quad [15]$$

$$CO(s) \leftrightharpoons CO(g) + (s) \quad [16]$$

The rate of carbon deposition would then depend on the net rate of dissociation of CO_2 and the net rate of adsorption and dissociation of CO species (steps [14]–[16]). Two kinds of carbon species can be identified in the TPH and TPO spectra of Figs. 5 and 6. The reactivity of these carbon species toward hydrogenation and oxidation is clearly higher than that corresponding to the carbon formed from CH_4 decomposition, as the TPH spectra of Figs. 2 and 5 illustrate. These results strongly suggest that the chemical structure of the carbon derived from CH_4 decomposition and CO_2 dissociation must be different. This, in turn, might imply that the Rh sites for carbon accumulation and the surface composition, which might affect carbon deposition, could be different. It is noted that during CH_4 decomposition the Rh surface is expected to be in a more reduced state than in the case of CO_2 dissociation. In the latter case, the presence of adsorbed oxygen species in an amount corresponding to $\theta_O = 0.74$, based on the TPO results of Fig. 6, may hinder the growth of adsorbed atomic carbon to whiskers or to the graphite form. It may also prevent transport of carbon on the alumina surface.

The relatively active form of carbon produced at 650°C after CO_2/He reaction, as deduced from the TPH and TPO results of Figs. 5 and 6 ($T_M = 150$°C), has also been observed by Efstathiou *et al.* (9–11) over 1 and 5 wt% Rh/Al_2O_3 catalysts during CO/H_2 and CO/He reactions in the range of 180–280°C. This carbon species is free of hydrogen and it is derived from the dissociation of adsorbed CO species. Of interest is the fact that aging of carbon derived from the dissociation of CO_2 at 650°C is rather limited as compared to the case of CH_4 decomposition (compare Figs. 2 and 5). *In situ* FTIR experiments performed over the present catalyst revealed that following CH_4/CO_2 reaction at 650°C, where CO/H_2 is produced, and a subsequent 10-min Ar purge at 650°C, no adsorbed CO exists (2). These results exclude the possibility that during the TPH and TPO experiments presented in Figs. 5 and 6 some of the CH_4 or CO_2 response is due to the hydrogenation or oxidation, respectively, of adsorbed CO species formed during CO_2/He reaction at 650°C.

The formation of carbon upon reaction of the Rh/Al_2O_3 surface with CO_2/He passes first through the formation of adsorbed CO, where the latter species can desorb into the gas phase as illustrated by the surface elementary reaction steps [14]–[16]. The transient of CO production during the 10-min CO_2/He treatment of the catalyst at 650°C could not be analyzed because of the following reason: The CO_2/He mixture used in the present study contained 20 mol% CO_2. As indicated by the amount of carbon formed, the corresponding concentration of CO_2 consumed is very small. Due to the fact that a large signal of 28 peak in the mass spectrometer was due to unreacted CO_2 (cracking of CO_2 to CO^+ ($m/z = 28$)), the additional small signal of 28 peak arising from the presence of CO in the CO_2/He reaction mixture could not be resolved after subtraction.

(c) Reaction of CH_4/CO_2 with Rh

A limited amount of fundamental work has been performed on the characterization (quantitative and qualitative) of carbonaceous species formed on supported Rh catalysts during reforming of CH_4 with CO_2 at temperatures higher than 600°C (1–3, 6, 12). Erdöhelyi *et al.* (6) have measured the amount of carbon accumulated on the surface of the 1 wt% Rh/Al_2O_3 catalyst upon CH_4/CO_2/He reaction at 500°C for 1 h. They found that this carbon amounts to only 0.07 monolayers, based on the fresh exposed surface area of Rh (before reaction studies).

The present TPH results shown in Fig. 7 and those reported in Tables 1 and 2 clearly demonstrate that, for

the present catalytic system and reaction conditions, three kinds of carbon species accumulated on the catalyst surface. A very active carbon species, C_α, is hydrogenated at 100°C, and this is probably of carbidic form, as observed also on Rh/Al_2O_3 following CO/He and CO/H_2 reactions (9–11). The amount of this very active C_α carbon species is found to be the largest at short times on stream (2 min) and the smallest at long times on stream (2 h) (see Table 1). A similar behavior was also observed for the second kind of carbon species C_β (second peak in the TPH spectrum of Fig. 7). Aging of carbon is, therefore, apparent from these results where the inactive carbon formed cannot be hydrogenated up to 500°C (compare results at 650°C in Tables 1 and 2). However, we have previously reported that this inactive carbon can be oxidized to CO_2 (1), whereas the total amount of carbon accumulated during reforming reaction, as measured by oxygen titration, stays practically constant with reaction time up to 2 h on stream (see Table 2, $T = 650$°C).

It is important to note that, based on previous *in situ* FTIR studies (2), the carbonate, formate, and CO adsorbed species formed during reforming reaction all desorb or decompose during the 10-min He purge at 650°C applied before initiation of the TPH experiments. In addition, we have also demonstrated that hydrogenation of carbonate species does not take place at temperatures below 500°C. Thus, the three CH_4 peaks observed in Fig. 7 correspond to a true hydrogenation process of different kinds of adsorbed carbon species.

In a recent work (2, 3) we have demonstrated, via isotopic experiments (use of $^{13}CH_4$ in the feed mixture), that the origin of carbon accumulated during reforming reaction in the range of 650–750°C over the Rh/Al_2O_3 catalyst is mainly that of the CO_2 molecular route (via CO dissociation), a result which suggests that the carbon species derived by the decomposition of CH_4 (steps [9]–[11]) are more active toward CO formation than carbon species derived from the CO_2 molecular route. In the TPH spectrum of Fig. 7 only the first CH_4 peak ($T_M = 100$°C) contains some carbon derived from CH_4 decomposition (3). On the other hand, in the case of Ni-based reforming catalysts, accumulated carbon is derived from both CH_4 and CO_2 molecules (13, 14). These results demonstrate the different chemistry and kinetics of carbon deposition and removal steps during reforming reaction of CH_4 with CO_2 over Rh versus Ni catalysts.

The results shown in Table 2 indicate a significant decrease of carbon accumulation by increasing temperature of reforming from 650 to 750°C. This result is suggested to be largely due to removal of carbon by steam, according to the following reaction:

$$C + H_2O \leftrightharpoons CO + H_2. \qquad [17]$$

Reaction [17] is expected to become more significant with increasing reaction temperature. Of course, one cannot exclude the possibility that the net rate of carbon formation, as determined by steps [14]–[16] (i.e., $C + CO_2 \leftrightharpoons 2CO$), decreases with increasing reaction temperature. In fact, the reaction of atomic carbon and oxygen (step [15]) to form CO becomes significant at high temperatures. The amount of carbon accumulated at 750°C was found to decrease with reaction time as shown in Table 2. This result suggests that, as far as the surface concentration of total carbon, there is no achievement of a steady-state condition after 2 h on stream. The active carbon participating in the formation of CO is less than 0.2 of a monolayer after 10 min of reforming reaction at 650°C, as measured by steady-state isotopic experiments (2). Therefore, part of the carbon reported in Tables 1 and 2 is a spectator species.

(d) Kinetics of Hydrogenation of Carbonaceous Species

The temperature-programmed hydrogenation experiments of the various carbonaceous species formed upon exposure of the catalyst to CH_4/He, CO_2/He, and CH_4/CO_2/He, presented in Figs. 2, 5, and 7, respectively, can be used to estimate an intrinsic activation energy of the hydrogenation process of the carbonaceous species based on well established TPH theory (15). The activation energy is defined by (15)

$$\frac{E_r - \frac{1}{2}\Delta H^o_{ads}}{RT_M^2} = \left(\frac{AH}{\beta}\right) \cdot e^{-E_r/RT_M} + \frac{5}{4} \cdot \frac{1}{T_M}, \qquad [18]$$

where E_r is the activation energy of hydrogenation (kJ/mol), ΔH^o_{ads} is the heat of adsorption of hydrogen (kJ/mol), A is the preexponential factor of the rate constant, k, of the rate-determining hydrogenation step ($cm^2/s \cdot site$), H is the hydrogen atom concentration at T_M (H atoms/cm^2), T_M is the peak maximum temperature (K), β is the linear heating rate (K/s), and R is the gas constant. In order to be able to calculate the value of E_r, the parameters ΔH^o_{ads}, A, and H must be known. The parameter A has a typical value of 10^{-2} (16) ($A = kT/hS$, where k is Boltzman's constant, h is Planck's constant, and S is the density of sites per cm^2). The heat of hydrogen adsorption used in the present work is an experimental one reported by Efstathiou and Bennett (17) for the Rh/Al_2O_3 catalyst, $\Delta H^o_{ads} = 62.7$ kJ/mol at $\theta_H = 0.8$ monolayers. The H value corresponding to the present clean Rh/Al_2O_3 catalyst at 300 K is estimated to be $H = 3.2 \times 10^{13}$ (H atoms/cm^2). However, this value is the maximum one experienced during the TPH experiments. The effect of this parameter on the resulting value of E_r is discussed later.

The intrinsic activation energies of the hydrogenation of the main carbon species formed (as deduced by TPH) upon CH_4/He, CO_2/He and CH_4/CO_2/He exposures at 650°C for 10 min are calculated employing Eq. [18]. The results are given in Table 3. The higher of the two values of E_r shown in Table 3 corresponds to the largest possible value of H,

TABLE 3

Intrinsic Activation Energies of the Hydrogenation of the Main Carbon Species Formed after Reaction with CH_4/He, CO_2/He, and CH_4/CO_2/He Mixtures at 650°C for 10 min

Reaction	T_M (K)	E_r (kJ/mol)
CH_4/He	973	230–250
CO_2/He	430	96–108
CH_4/CO_2/He	508	120–130

as discussed in the previous paragraph. However, at the T_M temperature not all the Rh surface is free for hydrogen chemisorption due to some carbon remaining on the surface. If it is assumed that the H value at T_M is 10 times lower than that corresponding to a clean surface, the lower value of E_r is obtained. Thus, Eq. [18] appears not to be very sensitive to the value of H assumed since the deviation of the value of E_r is less than 10% when the value of H is altered by one order of magnitude. It is also important to note that the initial concentration, C_o, of adsorbed carbon species (before the start of the TPH experiment) does not appear in Eq. [18]. Thus, even though the initial concentration of carbon in all three TPH experiments shown in Figs. 2, 5, and 7 is different, the estimated E_r values shown in Table 3 do not suffer from such discrepancy. On the other hand, it is true that the initial concentration of carbon may affect the concentration of sites of H_2 chemisorption, H, at T_M, and therefore, the estimate of E_r value according to Eq. [18]. However, as mentioned above, alterations in the estimation of E_r value are small by changing the H value by an order of magnitude. In addition, it can be easily shown via Eq. [18] that changes in the H value by an order of magnitude can cause a change in the observed T_M value by only about 20 K. This result also does not affect the estimated E_r value by more than 10%.

The magnitude of the activation energy of the hydrogenation of carbon species formed can be used to draw conclusions concerning their chemical structure. The high value of 230–250 kJ/mol must correspond to a graphite form of carbon (4), while the activation energy values in the range of 105–125 kJ/mol are typical values for the hydrogenation of carbon produced upon CO/H_2 and CO/He reactions over Group VIII metal catalysts (4). In the present case, this carbon is likely to be in the form of alkyl chains, practically free of hydrogen.

The similar activation energy values of the hydrogenation of the main carbon species formed upon CO_2/He and CH_4/CO_2/He reactions at 650°C, reported in Table 3, are in harmony with previously reported findings (2, 3) which demonstrated that the origin of this carbon species is mainly the CO_2 molecular route. More precisely, dissociation of adsorbed CO species, the latter formed via CO_2 dissociation, leads initially to carbidic carbon and oxygen atoms, while the carbidic carbon could be transformed into other, less active, forms as reforming reaction proceeds.

The transient isothermal hydrogenation results shown in Figs. 4 and 8 indicate that over a wide range of temperatures the maximum of the rate of hydrogenation of carbon to CH_4 appears at $t_m = 0$. This result implies that the kinetics of this hydrogenation process proceed with only one rate-limiting step according to results of kinetic modeling (18). On the contrary, the results of the transient isothermal oxidation experiments shown in Fig. 3a, $t_m \neq 0$, and according to Eq. [7] under Results reveal that more than one step could be considered as rate-limiting in the oxidation process.

(e) Kinetics of Oxidation of Carbonaceous Species

The kinetic model developed (described by Eqs. [1]–[8] and in the Appendix) explains well the experimental features of the transient isothermal oxidation experiments presented in Fig. 3a, as also illustrated in Fig. 3b by application of Eq. [8]. As discussed in the Appendix, Eq. [8] can be equally well applied in two cases: The first case is when the oxidation step of CH_x is the rate-limiting step ($\alpha > 1$, i.e., $\alpha = 10$, or $k_2 = 10k_1$), and the second case is when the oxidation of surface CO to CO_2 is the rate-limiting step ($\alpha < 1$, i.e., $\alpha = 1/10$, or $k_1 = 10k_2$). In the case when both steps have similar rate constants, i.e., $k_1 \cong k_2$ or $\alpha \cong 1$, the model predicts that the maximum of the rate of CO_2 formation occurs at times close to zero ($t_m \cong 0$). The present model and the experimental results do not distinguish among the first two cases. However, the good fit of the data to the model allows one to evaluate the activation energy of the rate-limiting step of the oxidation process. In the following, an attempt is made to relate the value of the activation energy obtained ($E = 63$ kJ/mol) to that corresponding to the carbon and CO oxidation steps over Rh surfaces, which have appeared in the literature.

The BOC-MP (bond order conservation–Morse potential) theoretical approach developed by Shustorovich (19) has been used with success to investigate the mechanism (sequence of elementary steps) of many catalytic systems (19–23). The heats of adsorption of all adsorbed species which participate in the reaction network, and the activation energies, ΔE^*, of all elementary reactions can be calculated. Here, we apply the BOC-MP method to examine the reaction of atomic carbon with oxygen to form adsorbed CO, and that of adsorbed CO with oxygen to form CO_2 on the Rh(111) surface.

Let us consider first the surface oxidation: $C(s) + O(s) \overset{\Delta E_1^*}{\rightarrow} CO(s) + (s)$, which proceeds with an activation barrier ΔE_1^*. Within the BOC-MP framework, in the zero coverage limit, the heats of adsorption of molecules and molecular fragments, Q, and the activation barriers of recombination of atomic or molecular species, ΔE^*, are calculated based

on Eqs. (A.1)–(A.10) reported elsewhere (23). The experimental values, Q_O and Q_{CO}, for adsorbed atomic oxygen and molecular CO are 426.4 kJ/mol (24) and 133.8 kJ/mol (25), respectively, while that of Q_C for carbon is assumed to be 668.8 kJ/mol (26). The gas-phase bond energy of CO, D_{CO}, determined experimentally, is 1074.3 kJ/mol (26). From these values and the equations mentioned above it is calculated that $\Delta E_1^* = 73.6$ kJ/mol. If it is assumed that $Q_C = 752.4$ kJ/mol, a value of $\Delta E_1^* = 121.2$ kJ/mol is estimated. On the other hand, a recent work of Mikhailov *et al.* (27) presents experimental evidence that the surface reaction step of the recombination of adsorbed atomic carbon on polycrystalline Rh ribbon with adsorbed atomic oxygen ($P_{O_2} = 8 \times 10^{-8}$ mbar) to form CO proceeds with an activation energy of about 167.2 kJ/mol. This relatively high value may be associated with a low surface oxygen coverage.

In the case in which the surface oxidation: $CO(s) + O(s) \overset{\Delta E_2^*}{\rightarrow} CO_2$ is considered, which proceeds with an activation barrier ΔE_2^*, the BOC-MP analysis provides a value of $\Delta E_2^* = 100.3$ kJ/mol. This value agrees very well with that reported experimentally ($\Delta E_2^* = 112.8$ kJ/mol, Ref. 28). However, at high oxygen surface coverages this energy barrier drops to as low as 50.2 kJ/mol (29).

The energy barrier ΔE_2^* for the surface oxidation of CO to CO_2 could also be estimated over polycrystalline supported Rh surfaces making use of kinetic information determined experimentally for this particular reaction. If one assumes that (a) the rate-determining step is the surface reaction of adsorbed CO and oxygen species, (b) adsorption of CO and O_2 are at equilibrium, and (c) the partial pressure of CO is small enough with respect to the oxygen pressure, then the apparent activation energy, determined from the rate equation of CO_2 formation, is

$$E_{app} = E_r + \Delta H^o_{CO} - \Delta H^o_{O_2}, \qquad [19]$$

where E_r is the intrinsic activation energy of the surface reaction step of adsorbed CO with adsorbed oxygen to form CO_2 (step [3]), and ΔH^o_{CO} and $\Delta H^o_{O_2}$ are the heats of adsorption of CO and O_2, respectively. Typical values for the heats of adsorption of oxygen and CO at small coverages are $\Delta H^o_{O_2} = -250$ kJ/mol and $\Delta H^o_{CO} = -125$ kJ/mol (30, 31). A typical value of the apparent activation energy of the CO oxidation reaction appears to be in the range of 105–125 kJ/mol (32). In the case in which the Rh surface is populated with adsorbed oxygen rather than CO species ($\theta_O \rightarrow 1.0$, $\theta_{CO} \rightarrow 0$), then $\Delta H^o_{O_2}$ could even be as low as 118 kJ/mol. Using the aforementioned values into Eq. [19] one finds that the value of E_r is of the order of 42–62 kJ/mol which agrees well with that mentioned in the previous paragraph for the Rh(111) surface.

In the present work, the experimental results of the oxidation of carbon species to CO_2 (Fig. 3a) must correspond to high surface oxygen coverages. The kinetic model developed to explain the features of the transient responses of the CO_2 formation resulted in an activation barrier of 63 kJ/mol if either one of the two elementary steps [2] or [3] is considered as rate-determining step. Following the discussion offered in the previous paragraphs, this value is reasonable for either elementary reaction step. Thus, it is not possible, using the information at hand concerning the activation barriers of each of the two reaction steps, to decide which step is the rate-determining one. It is also interesting to note that if both steps are considered to be rate-determining with $k_1 = k_2$ (or $\Delta E_1^* \cong \Delta E_2^*$), the kinetic model developed (Eq. [7]) predicts no shift in the peak maximum of the CO_2 response, a result different than that observed (Fig. 3a).

CONCLUSIONS

The following conclusions can be drawn from the results of the present investigation.

1. Decomposition of CH_4 from a 20% CH_4/He mixture at 650°C over Rh/Al_2O_3 proceeds with a high initial rate (TOF = 0.045 s^{-1}), resulting in H_2 gas and carbonaceous residues on the surface ($\theta_c = 8.1$ at $t = 10$ min). The chemical structure of these carbonaceous species was probed to be that of graphite or polymerized carbon which is hydrogenated exclusively to CH_4 with an activation energy of about 230 kJ/mol. In addition, these carbonaceous species are oxidized to CO_2 with an intrinsic activation energy of 63 kJ/mol, as deduced from a kinetic model and transient oxidation experiments.

2. Dissociation of CO_2 from a 20% CO_2/He mixture at 650°C over Rh/Al_2O_3 results in the formation of two types of carbon species (as deduced by TPH and TPO techniques) in an amount of $\theta_c = 0.37$ monolayers (at $t = 10$ min). Hydrogenation of the main carbon species proceeds with an activation energy of approximately 96 kJ/mol. Its structure is likely that of carbidic and/or small chains of carbon atoms.

3. The reforming reaction of methane with carbon dioxide at 650°C over the Rh/Al_2O_3 catalyst results in the accumulation of three kinds of carbon species (as deduced by the TPH technique). Transformation of the active form of carbon to less active forms occurs with increasing reaction time. However, the total amount of carbon stays practically constant with reaction time up to 2 h on stream ($\theta_c = 0.55$). Hydrogenation of the main carbon species formed proceeds with an activation energy of similar magnitude as that found in the case of the CO_2/He reaction. These results are in agreement with previous findings (2, 3) that the origin of carbon accumulated over the present Rh/Al_2O_3 catalyst is mainly the CO_2 molecular pathway and not the CH_4 molecular pathway. It is found that accumulation of carbon decreases at temperatures higher than 650°C probably because of the importance of the reactions: $C + H_2O \rightleftharpoons CO + H_2$ and $C + CO_2 \rightarrow 2CO$.

APPENDIX

The basic material balance equations describing the change, with respect to reaction time, of the concentration of adsorbed CH_x and CO intermediate species involved in reaction steps [2] and [3], given under Results, are the following:

$$-\frac{d\Theta_{CH_x}}{dt} = k_1 \cdot \Theta_{CH_x} \cdot \Theta_{O\text{-}s} \quad [20]$$

$$\frac{d\Theta_{CO\text{-}s}}{dt} = k_1 \cdot \Theta_{CH_x} \cdot \Theta_{O\text{-}s} - k_2 \cdot \Theta_{CO\text{-}s} \cdot \Theta_{O\text{-}s}. \quad [21]$$

Assuming that the $\Theta_{O\text{-}s}$ remains constant during the transient isothermal oxidation experiment, the $\Theta_{CH_x}(t)$ is easily obtained from Eq. [20]:

$$\Theta_{CH_x}(t) = \Theta^{o}_{CH_x} \cdot \exp(-k_1 \cdot \Theta_{O\text{-}s} \cdot t). \quad [22]$$

Substituting Eq. [22] into Eq. [21], $\Theta_{CO\text{-}s}(t)$ is obtained:

$$\Theta_{CO\text{-}s}(t) = \left(\frac{k_1 \cdot \Theta^{o}_{CH_x}}{k_1 - k_2}\right) \cdot [\exp(-k_2 \cdot \Theta_{O\text{-}s} \cdot t) - \exp(-k_1 \cdot \Theta_{O\text{-}s} \cdot t)]. \quad [23]$$

After substituting Eq. [23] into Eq. [4] (see Results), the transient rate of CO_2 formation is obtained (see Eq. [5]).

Equation [6] (see Results) shows that in the case in which the value of the ratio of $k_2/k_1 = \alpha$ becomes equal to one, then t_m becomes zero (no shift in the time of appearance of the maximum of the rate of CO_2 formation). Thus, reaction steps [2] and [3] could be considered to control the overall oxidation rate. On the other hand, if α is large enough, i.e., $\alpha = 10$, then it is reasonable to suggest that the reaction step with the smaller rate constant (in this case k_1) must be considered to practically control the rate of oxidation. Similarly, if $\alpha = 0.1$ then the reaction step associated with k_2 must be considered to be the rate-determining step.

Equation [8] (Results section) applies only if the ratio of $k_2/k_1 = \alpha$ stays practically constant in the temperature range investigated. Thus, it is important to work within a narrow range of temperatures in which this assumption is valid.

ACKNOWLEDGMENT

Financial support by the Commission of the European Community (Contract JOU2-CT92-0073) is gratefully acknowledged.

REFERENCES

1. Zhang, Z. L., Tsipouriari, V. A., Efstathiou, A. M., and Verykios, X. E., *J. Catal.* **158**, 51 (1996).
2. Efstathiou, A. M., Kladi, A., Tsipouriari, V. A., and Verykios, X. E., *J. Catal.* **158**, 64 (1996).
3. Tsipouriari, V. A., Efstathiou, A. M., Zhang, Z. L., and Verykios, X. E., *Catal. Today* **21**, 579 (1994).
4. Bartholomew, C. H., *Catal. Rev.-Sci. Eng.* **24**(1), 67 (1982). [and references therein].
5. Claridge, J. B., Green, M. L. H., Tsang, S. C., York, A. P. E., Ashcroft, A. T., and Battle, P. D., *Catal. Lett.* **22**, 299 (1993).
6. Erdöhelyi, A., Cserényi, J., and Solymosi, F., *J. Catal.* **141**, 287 (1993).
7. Efstathiou, A. M., Papageorgiou, D., and Verykios, X. E., *J. Catal.* **141**, 612 (1993).
8. Bennett, C. O., *in* "Catalysis under Transient Conditions" (A. T. Bell and L. L. Hegedus, Eds.), American Chemical Society Symposium Series, Vol. 178, p. 1. ACS, Wahsington, DC, 1982.
9. Efstathiou, A. M., and Bennett, C. O., *Chem. Eng. Commun.* **83**, 129 (1989).
10. Efstathiou, A. M., and Bennett, C. O., *J. Catal.* **120**, 118 (1989).
11. Efstathiou, A. M., Chafik, T., Bianchi, D., and Bennett, C. O., *J. Catal.* **148**, 224 (1994).
12. Rostrup-Nielsen, J. R., and Bak Hansen, J.-H., *J. Catal.* **144**, 38 (1993).
13. Swaan, H. M., Kroll, V. C. H., Martin, G. A., and Mirodatos, C., *Catal. Today* **21**, 571 (1994).
14. Goula, M., Lemonidou, A., and Efstathiou, A. M., *J. Catal.*, in press.
15. Bianchi, D., and Gass, J. L., *J. Catal.* **123**, 310 (1990).
16. Boudart, M., and Djéga-Mariadassou, G., *in* "Kinetics of Heterogeneous Catalytic Reactions." Princeton Univ. Press, Princeton, NJ, 1981.
17. Efstathiou, A. M., and Bennett, C. O., *J. Catal.* **124**, 116 (1990).
18. Bianchi, D., and Gass, J. L., *J. Catal.* **123**, 298 (1990).
19. Shustorovich, E., *Surf. Sci. Rep.* **6**, 1 (1986).
20. Shustorovich, E., and Bell, A. T., *J. Catal.* **113**, 341 (1988).
21. Shustorovich, E., and Bell, A. T., *Surf. Sci.* **248**, 359 (1991).
22. Bell, A. T., and Shustorovich, E., *Surf. Sci.* **235**, 343 (1990).
23. Shustorovich, E., and Bell, A. T., *Surf. Sci.* **253**, 386 (1991).
24. Fisher, G. B., and Schmeig, S. J., *Vacuum Sci. Technol.* **A1**, 1064 (1983).
25. Thiel, P. A., Williams, E. D., Yates, J. T., and Weinberg, W. H., *Surf. Sci.* **84**, 54 (1979).
26. Shustorovich, E., *Adv. Catal.* **37**, 101 (1990).
27. Mikhailov, S. N., van den Oetelaar, L. C. A., Brongersma, H. H., and van Santen, R. A., *Catal. Lett.* **27**, 79 (1994).
28. Weinberg, W. H., *Surf. Sci.* **128**, L224 (1983).
29. Ertl, G., *in* "Catalysis: Science and Technology" (J. R. Anderson and M. Boudart, Eds.), Vol. 5, Chap. 3. Springer, Berlin, 1983.
30. De Koster, A., and Van Santen, R. A., *Surf. Sci.* **233**, 366 (1990).
31. Commelli, G., Dhanak, V. R., Kiskinova, M., Pangher, N., Paolucci, G., Prince, K. C., and Rosei, R., *Surf. Sci.* **260**, 7 (1992).
32. Ioannides, T., Verykios, X. E., Tsapatsis, M., and Economou, C., *J. Catal.* **145**, 491 (1994) [and references therein].